IEEE Photonics Journal
An IEEE Photonics Society Publication

Low Power Consumption Mode Switch Based on Three-Dimensional Polymer Mach-Zehnder Interferometer

Volume 12, Number 3, June 2020

Jiawen Lv
Tianhang Lian
Baizhu Lin
Yue Yang
Yue Cao
Xianwang Yang
Yunji Yi
Fei Wang
Daming Zhang

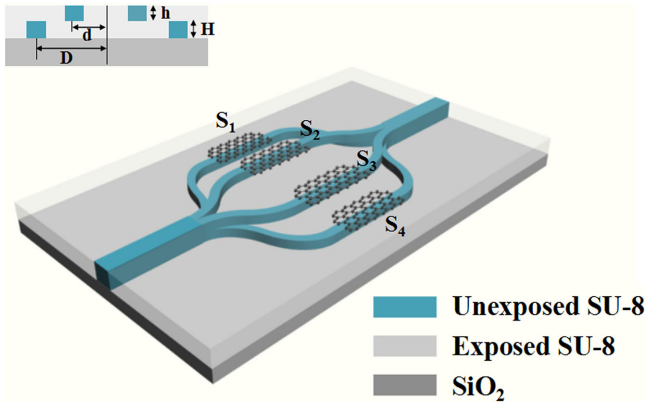

DOI: 10.1109/JPHOT.2020.2992745

Low Power Consumption Mode Switch Based on Three-Dimensional Polymer Mach-Zehnder Interferometer

Jiawen Lv, Tianhang Lian, Baizhu Lin, Yue Yang, Yue Cao, Xianwang Yang, Yunji Yi, Fei Wang, and Daming Zhang

State Key Laboratory of Integrated Optoelectronics, College of Electronic Science and Engineering, Jilin University, Changchun 130012, China

DOI:10.1109/JPHOT.2020.2992745

Manuscript received April 15, 2020; revised April 30, 2020; accepted May 3, 2020. Date of publication May 6, 2020; date of current version May 26, 2020. This work was supported in part by the Natural Science Foundation of Jilin Province under Grant 20190201190JC; in part the National Key R&D Program of China under Grant 2019YFB2203000, and in part the National Natural Science Foundation of China (NSFC) under Grant 61605057. Corresponding author: Yunji Yi (e-mail: yiyj@jlu.edu.cn).

Abstract: We present a polymer thermo-optic mode switch based on the structure of two vertical Mach-Zehnder interferometers (MZIs). It can achieve a rapid switch between E_{00}, E_{01}, E_{10} and E_{11} with the different heaters turning on. In our simulation, we compare two structures (the metal top electrode and the graphene electrode). The Finite element method (FEM) is used to simulate the parameters of the graphene electrode device. The power consumption of 1 and 3 heaters is 1.72 mW, and that of 2 and 4 heaters is 1.85 mW. In addition, the response speeds of the 1 and 3 graphene heater mode switch calculated are 36.9 μs (rise) and 103.4 μs (down), and that of 2 and 4 graphene heater mode switch calculated are 17.3 μs (rise) and 87.9 μs (down). The proposed model can be used in the field of low power consumption mode division and multiplexer of three-dimensional integrated.

Index Terms: The mode switch, Mach-Zehnder interferometers, photobleaching.

1. Introduction

Optical communication systems are developing rapidly, so people need to transmit and handle a lot of information. To meet these needs, it is necessary to increase the transmission capacity of photonic integration system further. Mode-division multiplexing (MDM) is a useful technique for improving the transmission capability of fiber-optic communication networks [1], [2]. It improves the transmission capacity of the fiber by controlling the number of patterns transmitted by independent signal channels, allowing different spatial modes of small mode fiber to carry different data channels. The mode switch is an essential component in an MDM system which can spatially combining or separating different mode channels [3], [4]. In MDM optical network, as a widely studied device, a mode switch has been deeply considered. Recent research issue is to realize multi-mode, high precision, and fast response under the limited waveguide size [5], [6].

Since the introduction of MDM, many technical solutions can implement modes multiplexing, demultiplexing, and conversion. In the early days, phase plates [7], [8] and spatial light modulators [9] were used to implement mode multiplexing and demultiplexing. However, these technical solutions are composed of discrete optical components, which are bulky and have high transmission losses,

and unsuitable for use in communication systems. Therefore, in order to fabricate devices that can be used in communication systems, researchers have begun to fabricate devices with compact structure and low transmission loss based on optical fibers or optical waveguides. There are some articles, the technical implementation of modular multiplexing is photonic lanterns [10], asymmetric Y branches [11], [12], long-period grating [13], [14], and directional couplers [15], [16], etc. On the other hand, waveguide multiplexers can be fabricated by using microfabrication technology based on lithography, which is more feasible, controllable, and easy integration. However, it is difficult for ordinary planar waveguide platforms to multiplex high-order fiber modes whose fields oscillate in the vertical direction. Therefore, there is an urgent need to research high-efficiency mode switches to transform a mass of spatial modes and achieve faster switching speed.

Recent studies have shown that three-dimensional (3D) structures can be particularly effective in controlling the spatial modes of an optical waveguide, such as structurally combined horizontal and vertical directional couplers [17], [18]. Such a three-dimensional waveguide multiplexer can be fabricated using polymers, and the preparation processes (such as spin coating and photolithography) are relatively easy to control. However, due to the absorption of the metal electrodes, cladding must exist between the electrode and waveguide core layer, which leads to the reported researches have low heating efficiency, large power consumption, and long response time. Graphene electrode was introduced to solve this problem, thermo-optic switch based on graphene electrode was proposed [19]. However, because of the existence of the upper cladding on the graphene layer, the switching time will be restricted. The reported structure needs the cladding to smooth the graphene and protect the graphene layer. In this letter, we designed a low power consumption and fast respond mode switch to implement a reconfigurable mode multiplexer. Embedded graphene electrode was introduced to eliminate the upper cladding, which ensured a fast switching speed and high heating efficiency. In addition, the electrode arrays can be fabricated in one step between two core layers with low light absorption, and the two waveguide core layers can protect the graphene. Third, the photobleaching technique will ensure a smooth layer surface and fast fabrication speed at low cost.

2. Design and Simulation

Our proposed mode switch consists of two vertically distributed Mach-Zehnder interferometers (MZIs). Each arm has an electrode corresponding to it, which is used to change the phase of the waveguide. A smooth surface can be obtained by the photobleaching process, which is convenient for electrode transfer and fabrication. We compared the two structures (the metal top electrode and the graphene electrode) and found that the graphene structure had better performance. Since graphene as an electrode can effectively reduce the absorption of light, we removed the upper cladding, which improves the heating efficiency of the electrode and reduces response time. Compared with the previously reported mode switch, our devices have lower power consumption and faster response times, which is of great significance for the implementation of MDM with rapid response.

Figure 1(a) shows a schematic diagram of the proposed 3D mode switch. The device consists of two vertically distributed symmetrical MZIs, each arm has an electrode for changing the phase of the waveguide. We have developed a photo-bleaching technology to fabricate 2D integrated mode switches, which can obtain smooth surfaces and adjustable refractive indices. According to different drying temperature, the refractive index of a photopolymer (SU-8) can be adjusted from 1.561 to 1.582 while the drying temperature vary from 150 °C to 190 °C [20]. The refractive index of UV-exposed SU-8 is 1.562, and the refractive index of the substrate is 1.45 [21]. The waveguide core layer is unexposed SU-8 with a refractive index of 1.582. Since the left and right arms of the upper and lower waveguides are symmetric, only one side of the waveguide is analyzed in this paper. Beam Propagation method (BPM) was used to scan the device parameters; the relationship between D and h was calculated, as shown in Fig. 2(a). In order to ensure that there is no phase difference caused by optical path difference between the upper and lower waveguides, and the power can be evenly distributed, D is set as 34.5 μm, H is set as 3 μm, d is set as 10 μm, and h is set as 2.04 μm. The size of the lower waveguide core is 3 μm $\times$ 3 μm, and the size of the

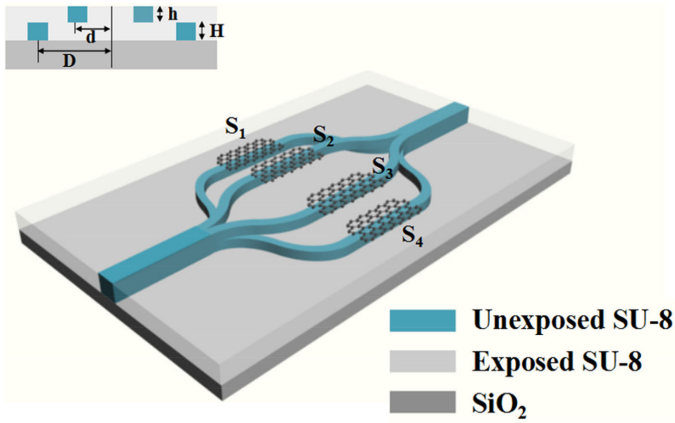

Fig. 1. Schematic diagram of the mode switch.

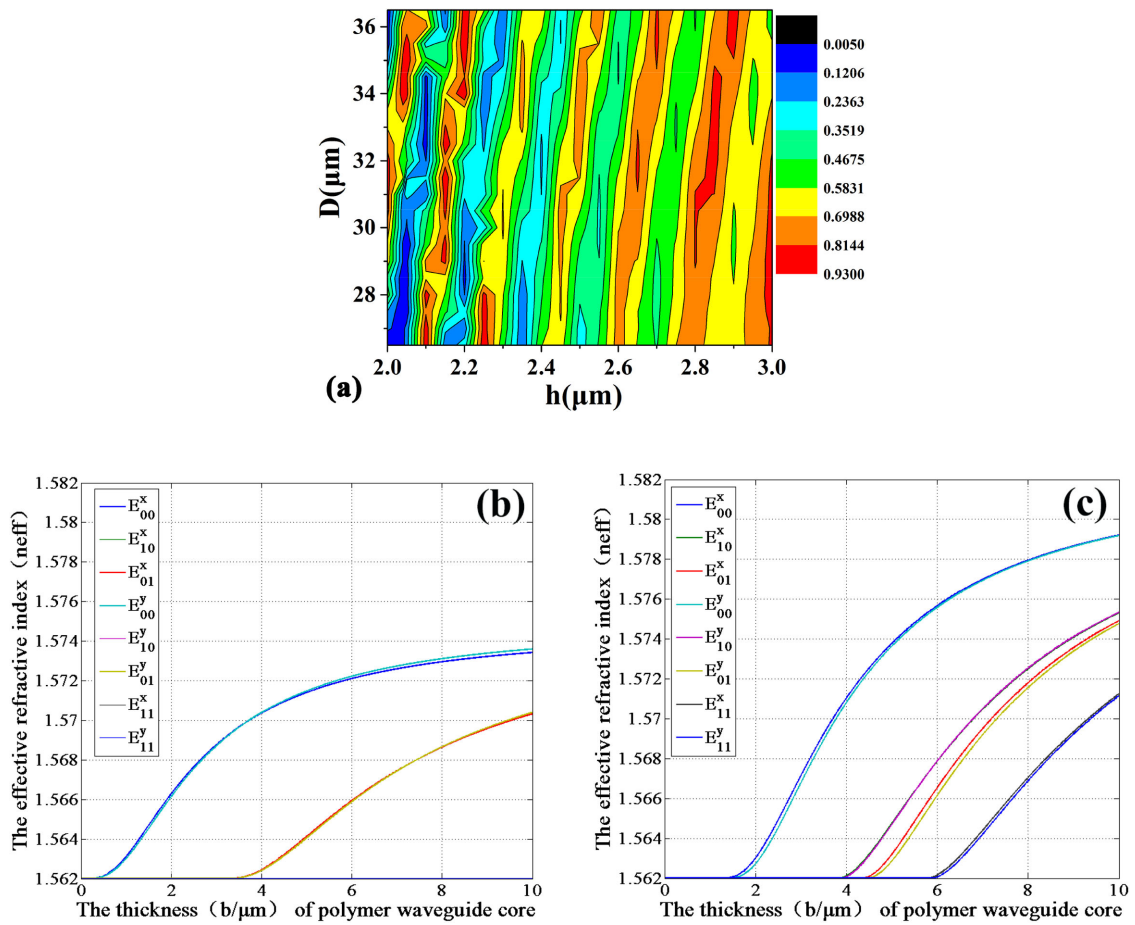

Fig. 2. Relationship between (a) the distance D, waveguide thickness h and output normalized power of the whole device, (b) the mode and waveguide the thickness h. (c) the mode and waveguide the thickness H.

TABLE 1
The Output of the Mode Switch in Different Cases

Input	Output			
	$S_1,S_2,S_3,$ S_4"off"	S_1,S_2"on" S_3,S_4"off"	S_1,S_3"on" S_2,S_4"off"	S_1,S_4"on" S_2,S_3"off"
E_{00}	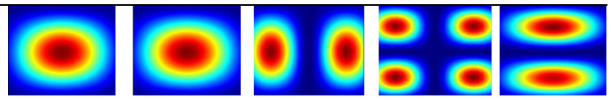			
E_{01}	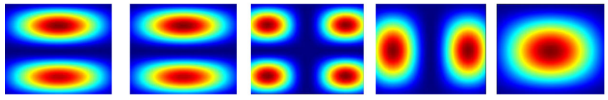			
E_{10}	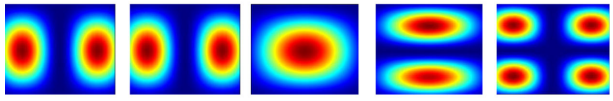			
E_{11}	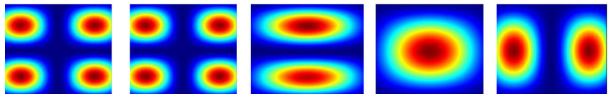			

upper waveguide core is 3 μm $\times$ 2.04 μm. The electrode length is 1 cm, and the total length of the device is 2 cm. Under this condition, MATLAB was used to calculate the relationship between size and mode, as were shown in Fig. 2(b) and 2(c), all the four branch arms are fundamental mode waveguide.

When the signal light with a wavelength of 1550 nm is launched from one side of the device, its light field is spatially divided into four equal parts. Since the branch arms of the MZI only support fundamental mode, it will be coupled to the E_{00} modes after passing through the Y-junctions. Then these fundamental modes propagate in the respective arms of the MZI and combine together. The output field pattern depends on the heating of the upper electrode heaters of the four branch arms. When all the four electrodes are not heated, there is no phase difference between the branch arms, and the output mode is the same as the input mode. When one of the electrodes is heated, there is a phase difference due to the thermo-optical effect. When the phase conversion of π is realized, it produces an extinction function and outputs a different field pattern. For example, when S_1 and S_2 are "on", S_3 and S_4 are "off", it makes the left and right half of the light field produce a phase difference of π at the output end. The E_{00} mode will be converted into E_{10}. With this same combination of electrode heating, changing the input light mode, it can also allow the conversion between the E_{01} mode and E_{11} mode. Changing the combination of electrode heating, this structure can realize the conversion between other modes. The specific electrode operation and output results are shown in Table 1.

The optical field distributions of two waveguides were calculated by the finite element method (FEM), respectively. The input optical signal is redistributed into four new fundamental modes when passing through the Y-junctions. Fig. 3(a) and (b) show the simulated light field diagrams of the two arms of the upper and lower layers of the mode switch. The light field is concentrated in the center of the waveguide and the scattering and absorption loss in the optical switch are low. The total loss of the switch is -0.46 dB, which is caused by Y-junctions and the S-bends.

Thermal conductivity of the mode switches can be evaluated according to the thermal field distribution of the waveguide. The heating efficiency of the electrode can reflect the power consumption of the device. In order to calculate the heating efficiency of the proposed switch, we simulated the

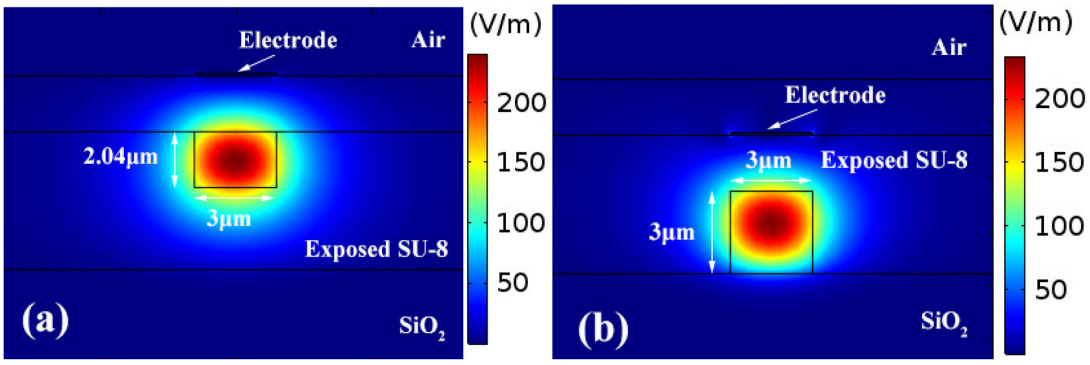

Fig. 3. Simulated light field diagram of (a) the upper waveguide and (b) the lower waveguide.

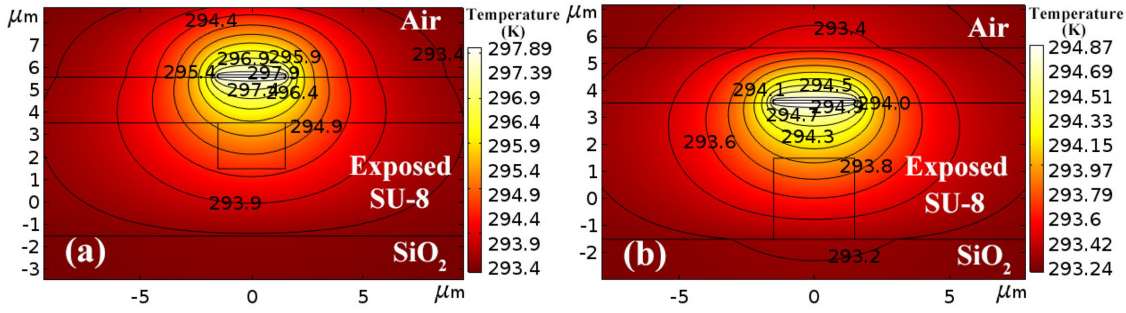

Fig. 4. FEM thermal simulation diagram of (a) the upper waveguide and (b) the lower waveguide of the top electrode structure.

thermal field of the upper and lower layers at the π phase shift by FEM, the results are shown in Fig. 4. For the upper waveguide, the thermal field distribution is shown in Fig. 4(a), when the electrode temperature is 298.145 K, the temperature of the waveguide core layer is 295.116 K. For the lower waveguide, as is shown in Figure 4(b), when the electrode temperature is 294.965 K, the temperature of the waveguide core layer is 293.598 K. We defined the heating efficiency of the electrode as α, according to Eq. 1 [22], we can calculate the heating efficiency of the two layers, respectively. When the initial temperature (T_0) is 293.15 K, the heating efficiency of the upper waveguide is calculated to be 39.36%, and the lower waveguide is 24.68%.

$$\alpha = \frac{T_{core} - T_0}{T_{electrode} - T_0} \tag{1}$$

Polymer materials have a higher thermo-optical coefficient than inorganic materials, which enables the mode switch to have a large effective refractive index change even the temperature change is small, thus reducing the power consumption. By changing the heating temperature of the electrode, the effective refractive index of the waveguide can be changed. When the phase changes π, the switching function can be realized, and the power consumption of the mode switch can be calculated. The heating power consumption of the mode switch can be calculated by Eq. 2 [23]. The power consumption of the upper waveguide and lower waveguide is 14.74 mW and 5.36 mW, respectively.

$$\Delta T' = \frac{\frac{P}{L}}{K\left(\frac{w}{t} + 0.88\right)} \tag{2}$$

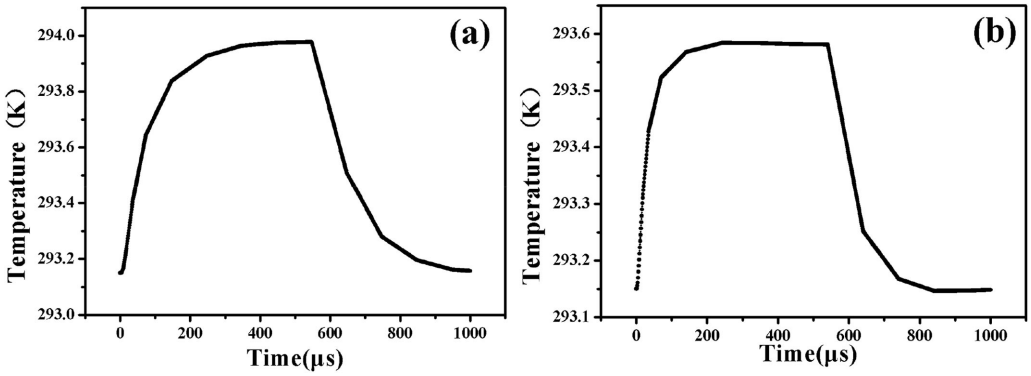

Fig. 5. The switching time of (a) the upper waveguide and (b) the lower waveguide of the top electrode structure.

FEM was used to calculate the time-domain response of the mode switch. By adding rectangular waves to the heaters, the switch can be turn on and off, then we can simulate two transient thermal simulations. The simulation results, as are shown in Fig. 5, are the switching times of the upper waveguide and lower waveguides, respectively. The temporary switching characteristic of the upper waveguide is shown in Fig. 5(a), from which the responce time of the mode switch is 192.3 μs (rise) and 238.4 μs (fall), respectively. Similarly, the temporary switching characteristics of the lower waveguide is shown in Fig. 5(b), from which the responce time of the switch is 90.4 μs (rise) and 156.8 μs (fall), respectively.

The structure of the top electrode has an upper cladding layer between core of the waveguide and Al electrode, which can reduce the absorption of the signal light by the electrode. However, a quantity of heat dissipates into the upper cladding layer, which entails lower heating efficiency. Previous studies have confirmed the possibility of graphene as an electrode, and graphene has low light absorption for TM mode. Therefore we propose a structure using graphene as an electrode. The structure removes the upper cladding layer and places the graphene electrode directly above the core layer of waveguide, which not only improves the heating efficiency of the electrode, but also reduces the switching time. The fabrication method of photobleaching can make the waveguide surface smooth, which is conducive to the transfer and fabrication of graphene. This method dramatically improves the possibility of the device in actual production.

Due to the removal of the upper cladding, the effective refractive index of the upper waveguide is changed. In order to ensure the equal power of the upper and lower waveguides, we only optimized the size of the upper and lower waveguides on the premise that the total size remains unchanged. We used BPM to rescan the dimensions of the device, and the output results are shown in Fig. 6(a). When h equals to 2.66 μm and D equals to 26.5 μm, the power of the four branch arms could be evenly distributed, and there is no phase difference between the upper and lower waveguides. At the same time, we used MATLAB to confirm a fundamental mode waveguide by calculating the relationship between size and waveguide mode, as is shown in Fig. 6(b) and (c). Under the above conditions, we used FEM to simulate the light field of the structure. We added a monolayer graphene above the waveguide core layer, with a width of 3 μm, a thickness of 0.34 nm. The refractive index of graphene is $2.52 + 2.24i$ at the wavelength 1550 nm [24], [25]. The simulation results are shown in Fig. 7(a) and (b), the light field is concentrated in the center of the waveguide. The total loss of the switch is -0.43 dB, which is caused by Y-junctions and the S-bends.

The thermal field distribution of the waveguides were simulated by FEM, and the results are shown in Figure 8. For the upper waveguide, when the electrode temperature is 293.579 K, The temperature of the core layer is 293.424 K, and the heating efficiency is calculated using Eq. 1, which are 63.87%. For the lower waveguide, when the electrode temperature is 293.582 K, The temperature of the core layer is 293.377 K, and the heating efficiency is calculated using

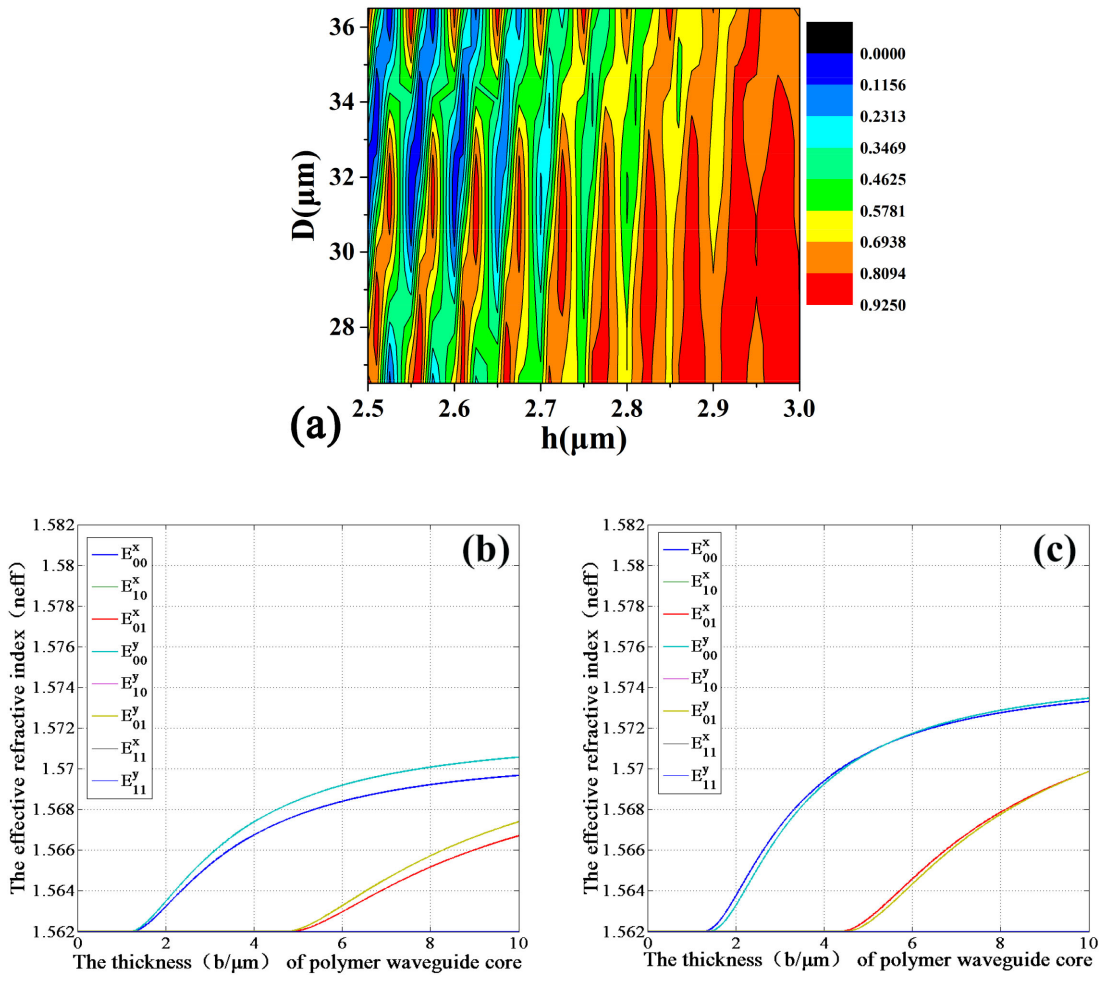

Fig. 6. Relationship between (a) the distance D, waveguide thickness h and output normalized power, (b) the mode and waveguide the thickness h. (c) the mode and waveguide the thickness H.

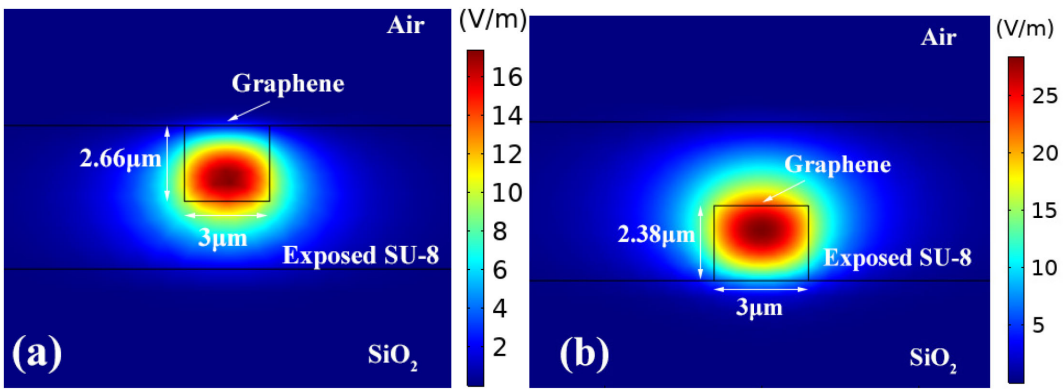

Fig. 7. Calculated light field distribution of (a) the upper waveguide and (b) the lower waveguide of the graphene electrode.

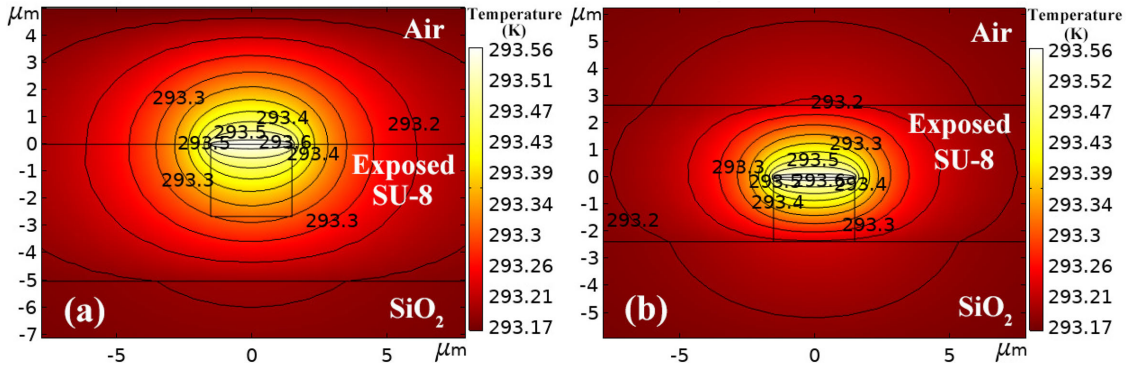

Fig. 8. FEM thermal simulation diagram of (a) the upper waveguide and (b) the lower waveguide of the graphene electrode structure.

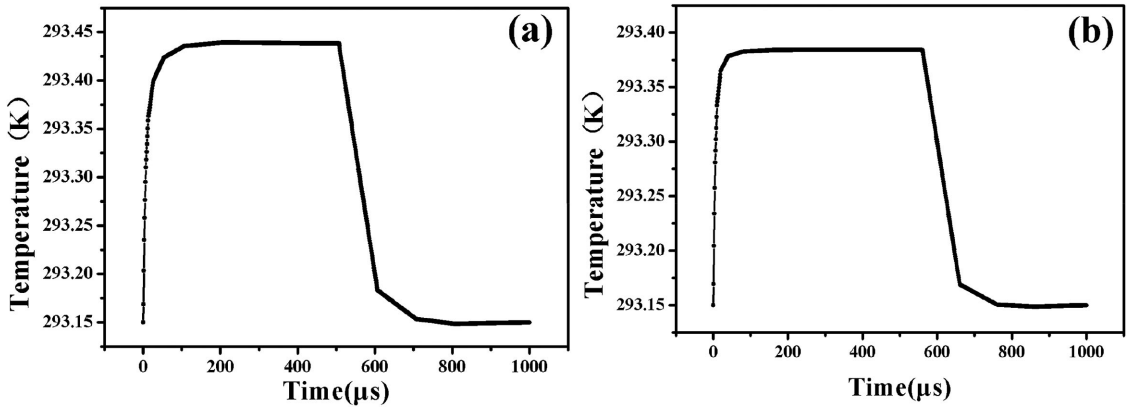

Fig. 9. The switching time of (a) the upper waveguide and (b) the lower waveguide of the graphene electrode structure.

Eq. 1, which are 52.55%. Compared with the top electrode structure, the heating efficiency is improved by 24.51% and 27.87%, respectively. Using Eq. 2, the power consumption of the upper and lower layers of the waveguide is calculated to be 1.72 mW and 1.85 mW, respectively. The power consumption of the device is significantly reduced.

We used FEM to calculate the time domain response of the graphene electrode structure by adding a rectangular square wave. Two transient thermal simulations, as shown in Fig. 9, are the switching times of the upper waveguide and lower waveguide, respectively. The temporary switching characteristic of the upper waveguide is shown in Fig. 9(a), from which the responce time of the switch is 36.9 μs (rise) and 103.4 μs (fall), respectively. Similarly, the temporary switching characteristic of the lower waveguide is shown in Fig. 9(b), from which the responce time of the device is 17.3 μs (rise), and the fall time is 87.9 μs (fall), respectively.

The more complex the structure is, the more difficult it is actually to fabricate the device. In order to simplify the fabrication process, we only changed the position of the graphene electrode of the upper waveguide, and placed it under the waveguide core layer (in the same plane as the lower graphene electrode), so that the electrodes can be fabricated in one time. FEM is used to simulate the performance of the upper waveguide, and the result is shown in Fig. 10. The heating efficiency is 52.45% and the power consumption is 3.28 mW. The temporal switching characteristic is shown in Fig. 10(c), from which the responce time of the switch is 52.0 μs (rise) and 130.8 μs (down), respectively. The performance of the structure is worse than that before the change, and

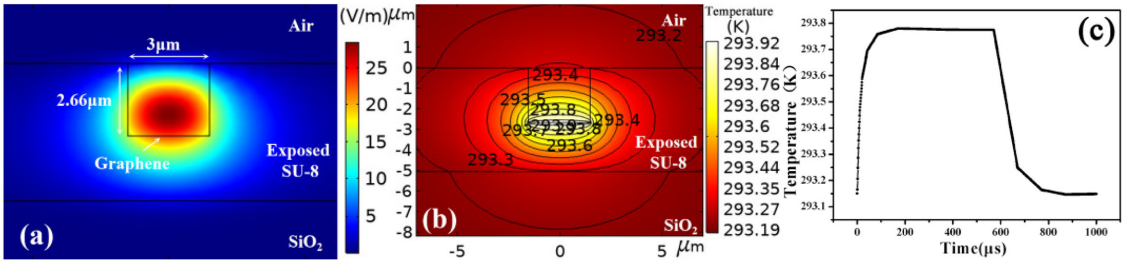

Fig. 10. Simulation results of (a) optical field, (b) thermal field, and (c) respond time of the switch.

the electrode of the structure absorbs more light due to the asymmetry of light field distribution. In the actual fabrication process, it can be selected according to the actual situation.

3. Conclusions

In conclusion, we have presented a 3D thermo-optic mode switch based on the structure of two vertical MZIs where four electrode heaters are fabricated on the four waveguides, respectively. By turning on the different heaters, it can achieve different outputs such as E_{00}, E_{01}, E_{10}, and E_{11}. FEM was used to calculate that the power consumption is 1.72 mW for the upper waveguide. The responce time of the presented switch is 36.9 μs (rise) and 103.4 μs (down), respectively. For the lower waveguide, the power consumption of the mode switch is 1.85 mW. The responce time of the switch is 17.3 μs (rise) and 87.9 μs (down), respectively. The proposed model may be a significant part for MDM applications to develope more effictive mode-controlling devices.

References

[1] T. Mizuno, H. Takara, A. Sano, and Y. Miyamoto, "Dense space-division multiplexed transmission systems using multi-core and multi-mode fiber," *J. Lightw. Technol.*, vol. 34, no. 2, pp. 582–592, 2016.
[2] T. Mizuno and Y. Miyamoto, "High-capacity dense space division multiplexing transmission," *Opt. Fiber Technol.*, vol. 35, pp. 108–117, 2017.
[3] G. Yin *et al.*, "Multi-channel mode converter based on a modal interferometer in a two-mode fiber," *Opt. Lett.*, vol. 42, no. 19, pp. 3757–3760, 2017.
[4] Y. Gao *et al.*, "A Degenerate-mode-selective coupler for stable DSP-free MDM transmission," *J. Lightw. Technol.*, vol. 37, no. 17, pp. 4410–4420, 2019.
[5] P. Gregg, P. Kristensen, A. Rubano, S. Golowich, L. Marrucci, and S. Ramachandran, "Enhanced spin orbit interaction of light in highly confining optical fibers for mode division multiplexing," *Nat. Commun.*, vol. 10, no. 1, pp. 1–8, 2019.
[6] A. Gatto, M. Rapisarda, P. Parolari, and P. Boffi, "Discrete multitone modulation for short-reach mode division multiplexing transmission," *J. Lightw. Technol.*, vol. 37, no. 20, pp. 5185–5192, 2019.
[7] V. A. J. M. Sleiffer *et al.*, "73.7 Tb/s (96 $\times$ 3 $\times$ 256-Gb/s) mode-division-multiplexed DP-16QAM transmission with inline MM-EDFA," *Opt. Express*, vol. 20, no. 26, pp. B428–B438, 2012.
[8] K. Igarashi, D. Souma, K. Takeshima, and T. Tsuritani, "Selective mode multiplexer based on phase plates and Mach-Zehnder interferometer with image inversion function," *Opt. Express 23*, vol. 23, no. 1, pp. 183–194, 2015.
[9] C. Koebele *et al.*, "Two mode transmission at 2 $\times$ 100 Gb/s, over 40 km-long prototype few-mode fiber, using LCOS-based programmable mode multiplexer and demultiplexer," *Opt. Express*, vol. 19, no. 17, pp. 16593–16600, 2011.
[10] N. M. Mathew, J. B. Christensen, L. Grüner-Nielsen, M. Galili, and K. Rottwitt, "Air-cladded mode-group selective photonic lanterns for mode-division multiplexing," *Opt. Express*, vol. 27, no. 9, pp. 13329–13343, 2019.
[11] J. D. Love and N. Riesen, "Single-, few-, and multimode Y-junctions," *J. Lightw. Technol.*, vol. 30, no. 3, pp. 304–309, 2011.
[12] W. Chen, P. Wang, and J. Yang, "Mode multi/demultiplexer based on cascaded asymmetric Y-junctions," *Opt. Express*, vol. 21, no. 21, pp. 25113–25119, 2013.
[13] A. Li, X. Chen, A. Al Amin, J. Ye, and W. Shieh, "Space-division multiplexed high-speed superchannel transmission over few-mode fiber," *J. Lightw. Technol.*, vol. 30, no. 24, pp. 3953–3964, 2012.
[14] W. K. Zhao, J. Feng, K. X. Chen, and K. S. Chiang, "Reconfigurable broadband mode (de) multiplexer based on an integrated thermally induced long-period grating and asymmetric Y-junction," *Opt. Lett.*, vol. 43, no. 9, pp. 2082–2085, 2018.
[15] X. Zi, L. Wang, K. Chen, and K. S Chiang, "Mode-selective switch based on thermo-optic asymmetric directional coupler," *IEEE Photon.Technol. Lett.*, vol. 30, no. 7, pp. 618–6215, 2018.

[16] Q. Huang, Y. Wu, W. Jin, and K. S. Chiang, "Mode multiplexer with cascaded vertical asymmetric waveguide directional couplers," *J. Lightw. Technol.*, vol. 36, no. 14, pp. 2903–2911, 2018.
[17] Y. Wu and K. S. Chiang, "Ultra-broadband mode multiplexers based on three-dimensional asymmetric waveguide branches," *Opt. Lett.*, vol. 42, no. 3, pp. 407–410, 2017.
[18] A. M. Velazquez-Benitez *et al.*, "Six mode selective fiber optic spatial multiplexer," *Opt. Lett.*, vol. 40, no. 8, pp. 1663–1666, 2015.
[19] X. B. Wang, W. Jin, Z. Chang, and K. S. Chiang, "Buried graphene electrode heater for a polymer waveguide thermo-optic device," *Opt. Lett.*, vol. 44, no. 6, pp. 1480–1483, 2019.
[20] X. B. Wang, J. Sun, C. M. Chen, X. Sun, F. Wang, and D. M. Zhang, "Thermal UV treatment on SU-8 polymer for integrated optics," *Opt. Mater. Express*, vol. 4, no. 3, pp. 509–517, 2014.
[21] J. Y. Chen and D. Gao, "A silicon-based compact triplexer using Bragg grating assisted non-reciprocal single microring resonator," *Opt. Laser. Technol.*, vol. 124, 2020, Art. no. 105971.
[22] Y. Cao *et al.*, "Polymer/glass hybrid DC-MZI thermal optical switch for 3D-integrated chips," *RSC Adv.*, vol. 9, no. 19, pp. 10651–10656, 2019.
[23] Y. F. Liu *et al.*, "Thermal field analysis of polymer/silica hybrid waveguide thermo-optic switch," *Opt. Commun.*, vol. 356, pp. 79–83, 2015.
[24] S. A. Mikhailov and K. Ziegler, "New electromagnetic mode in graphene," *Phys. Rev. Lett.*, vol. 99, no. 1, pp. 016803.1–016803.4, 2007.
[25] X. T. Gan *et al.*, "Graphene-assisted all-fiber phase shifter and switching," *Optica*, vol. 2, no. 5, p. 468, 2015.